Hindawi
Geofluids
Volume 2022, Article ID 9167573, 13 pages
https://doi.org/10.1155/2022/9167573

*Research Article*

# Experimental Investigation of the Influence of the Anchor Cable Inclination Angle on the Seismic Response Characteristics of Anchored Piles

**A. Fa-you**,[1,2] **Xue-gang Dai**,[1] **Peng ZHang**,[1] **Ming-chang Hei**,[3] **and Shi-qun Yan**[1]

[1]*Faculty of Land Resource Engineering, Kunming University of Science and Technology, Kunming, Yunnan 650093, China*
[2]*Key Laboratory of Geohazard Forecast and Geoecological Restoration in Plateau Mountainous Area, Ministry of Natural Resources of the People's Republic of China, Kunming, Yunnan 650000, China*
[3]*State Key Laboratory of Hydraulics and Mountain River Engineering, College of Water Resource and Hydropower, Sichuan University, Chengdu Sichuan 610065, China*

Correspondence should be addressed to A. Fa-you; afayou@163.com

Received 13 April 2022; Revised 27 May 2022; Accepted 6 June 2022; Published 24 June 2022

Academic Editor: Zizheng Guo



Studies show that prestressed anchor cable antislide piles have good antiseismic characteristics. As an important parameter in the design of anchor-cable piles, the effect of anchor-cable inclination on the seismic response of the anchor-cable pile system has been rarely studied so far. In the present study, the seismic response characteristics of the anchor-pulled pile under different cable inclinations are studied using a large-scale seismic model test platform and numerical methods. The obtained results show that the inclined angle of the anchor cable has a great influence on the seismic response of the pile-anchor system. It is found that under the same seismic conditions, the axial force of the anchor cable becomes smaller as the anchor dip angle increases, while the pile top displacement becomes larger. The dynamic earth pressure behind the pile changes from the sliding surface to the pile top, indicating that the earth pressure near the sliding surface and the pile top is of active and passive earth pressure types, respectively. This pressure decreases with the increase of the anchor dip angle, thereby affecting the performance of the antisliding pile.

## 1. Introduction

Antislide piles can be mainly divided into composite and noncomposite piles according to the combination form with other structures. A noncomposite pile generally refers to a single pile, independent of other structures. On the other hand, a composite pile, such as a prestressed anchor cable antislide pile, refers to a single pile combined with other structures. As a common slope reinforcement measure, the prestressed anchor cable antislide pile has superior characteristics, including low cost and quick construction, so it has been widely used in large-scale and extra-large slopes and reinforcement of landslide optimization [1–7]. Analyzing the damages of Wenchuan earthquake showed that the slope reinforced by a prestressed anchor cable antislide pile has promising antiseismic capabilities [8, 9].

With the rapid development of industrialization, numerous investigations from different aspects have been carried out on the seismic behavior of antislide piles. In order to investigate the seismic characteristics of noncomposite piles, Valsangkar et al. [10] performed shaking table tests on the seismic response of partially supported single piles and achieved earlier research time, accordingly. Moreover, Makris and Badoni [11] studied the nonlinear seismic response of single piles. He et al. [12] studied the three-dimensional limit analysis of seismic displacement of slope reinforced by piles. Sáez et al. [13] studied the seismic response of pile-supported excavation in the Santiago gravel stratum. Qu et al. [14] analyzed the seismic response characteristics of the antislide pile using the elastic-plastic theory. Li et al. [15] performed shaking table tests and studied the seismic response of landslides reinforced by minipiles. Zhang et al.

[16] carried out large-scale shaking table tests to study the seismic behavior of the pile-foundation slope of the antislide pile-reinforced bridge. It is worth noting that the seismic analysis of these noncomposite piles provides a basis to study composite piles. To study the seismic characteristics of the combination of anchor-pull piles, Su and Zhang [17] studied the influence of rock excavation blasting vibration on the prestressed anchor cable on the high and steep slope of the diversion tunnel of the Zipingpu project. Then Yang et al. [18] analyzed the dynamic response characteristics of anchor cables under a blasting load. However, further investigations revealed that there are essential differences between blasting vibration and earthquake. Accordingly, the abovementioned analyses cannot be applied to the seismic design of the prestressed anchor cable. Ye et al. [19] carried out shaking table tests of slope reinforced by single-row antislide pile and prestressed anchor cable under the earthquake action. Lederer et al. [20] studied the interaction between embedded an antislide pile and a prestressed anchor frame beam. Qu et al. [21] studied the earth pressure distribution on different parameters, including the seismic response characteristics of the pile displacement, prestress of the anchor cable, dynamic characteristics and acceleration amplification effect of the reinforced slope, and seismic response of an antislide pile with anchor cable. Zhou et al. [22] and Yan et al. [23] analyzed the ultimate strength and anchorage characteristics of prestressed anchor cable in bedding rock slope. Fu et al. [24] carried out the shaking table test and studied the seismic response of slope reinforced by a pile-cable support structure. Furthermore, Chen et al. [25] studied the influence of earthquake characteristics on the seismic performance of anchored sheet pile quay with barrette piles. Lin et al. [26] studied the seismic response of beam-sheet-pile walls with anchor frames numerically and experimentally. Huang et al. [27] simulated the seismic response and failure mode of slope reinforced by the pile-anchor structure. It should be indicated that although the seismic study of these composite structures with anchor-pull piles provides a theoretical basis for the seismic design of composite structures, the influence of anchor cable inclination angle on the seismic response of anchor-pull pile composite structures is often neglected in the calculations, thereby affecting the accuracy of the results.

Reviewing the literature indicates that as an important parameter in the design of anchor-cable pile, the effect of anchor-cable inclination on the seismic response of the anchor-cable pile system has not yet been studied so far. More specifically, most investigations in this area only consider the influence of static action on the prestressed anchor-cable inclination [1, 2, 7]. Accordingly, it is of great theoretical value to study the seismic response of antislide piles with different inclination angles by performing shaking table tests and provide a scientific basis to improve and develop the aseismic design method of the anchor cable antislide pile.

## 2. Model Design

*2.1. Similarity Principle.* According to similarity criteria, the similarity of physical variables can be mainly divided into three categories, including general geometric similarity, dynamic similarity, and kinematic similarity. General geometric similarity refers to elementary geometric similarity wherein the unit length is generally considered the dimension of physical variables. Combining similar characteristics of various physical systems, the positions and significances of three categories can be described as that if any two systems are similar in geometry, dynamics, and kinematics, then the two systems have similar performances [28]. It is worth noting that among the three similarity criteria, the geometric similarity is easier to be achieved while reaching both the geometric and dynamic similarity is required to have the kinematic similarity. Accordingly, it is a challenge to reach the kinematic similarity in complicated engineering problems. Any solution obtained from the dynamic similarity under the condition of geometric similarity should satisfy the requirements of the kinematic similarity.

In the present study, the geometric and dynamic similarity of the anchor-pull pile supporting landslides is used as the basic conditions. Due to limited data on the properties of the prototype materials, including the standard values of the characteristic parameters, it is an enormous challenge to achieve complete similarity between the model materials and the prototype materials. Consequently, it is a challenge to reach an agreement between the test results and the prototype results. Aiming at resolving this problem, the main objective of the present study is to study the similarity laws in the test model.

*2.2. Experimental Equipment.* In the present study, tests are performed on the large shaking table (Yunnan Institute of Engineering Aseismic, China). The table size was 4 m × 4 m and has 3 degrees of freedom. The table can supply a maximum of 30 tons of load in the test. The maximum displacement and velocity along the $X$ and $Y$ directions are 250 mm and 0.8 m/s, respectively. Moreover, the maximum acceleration along the $X$ and $Y$ directions with a load of 20 and 30 tons is 1 g and 0.8 g, respectively. The operating frequency is 0~100 Hz, and the maximum overturning moment is 300 KN m.

Numerous materials, including landslide material, model box, retaining plate, antislide pile, anchor cable, and concrete, are involved in the test. The landslide model consists of three parts, including the sliding bed, sliding surface, and sliding body. Silty clay is used as soil. The sliding-bed soil is compacted before the test. To prepare the sliding surface, the soil is first screened with a 2 mm sieve. The screened soil is then dried; impurities are picked out and mixed with 50% fine sandy soil. The prepared sliding surface soil is evenly distributed over the sliding bed with a thickness of 5 cm. Natural-grade silty clay is used as the sliding soil. Instead of sieving, drying, and tamping, the silty clay is stacked above the sliding surface and leveled evenly. The bedrock of the anchoring section of the antislide pile is made of C40 concrete. Table 1 shows the physical and mechanical parameters of the test material.

A 60 cm long wooden antislide pile with a cross-section of 80 mm × 80 mm is used in the tests. The bottom is

Table 1: Physical and mechanical parameters of the test material.

| Material | $r$ kN/m$^3$ | $Es$ MPa | $\mu$ | Cohesion c kPa | Internal friction angle $\varphi$ ° |
|---|---|---|---|---|---|
| Sliding body | 19 | 20 | 0.30 | 8 | 12 |
| Sliding surface | 18.8 | 20 | 0.30 | 10 | 8 |
| Sliding bed | 21 | 35 | 0.25 | 15 | 14 |
| C40 | 24.4 | 3.25$E$4 | 0.2 | Elastic material | |

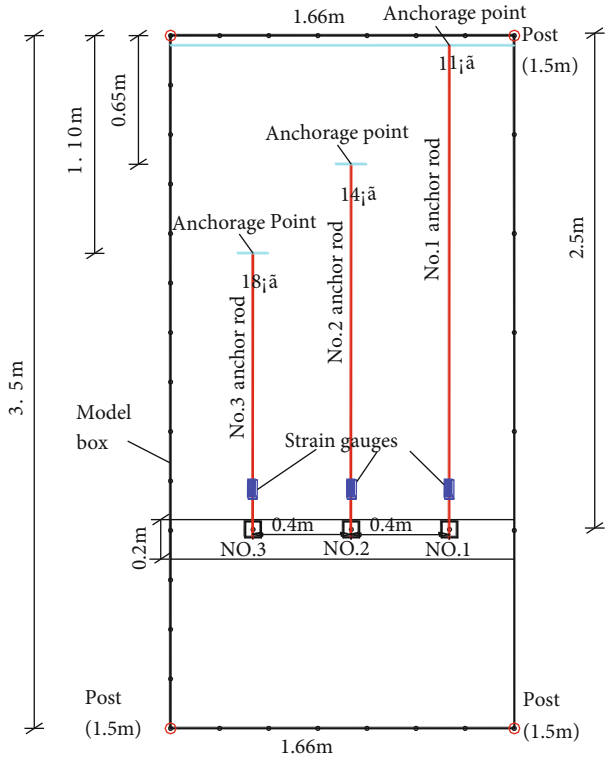


Figure 1: Top view of the physical model.

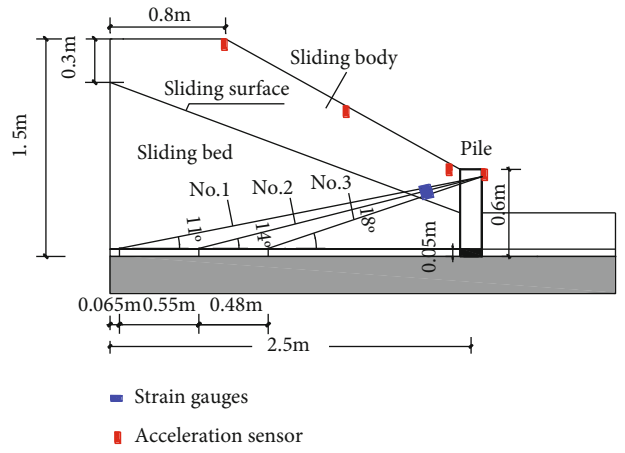


Figure 2: Schematic of the physical model.


Figure 3: Assembly of the acceleration sensors.

embedded in the concrete cast in a steel channel as the rock-socketed depth of the antislide pile. Each antislide pile has a 15 mm diameter hole at 5 cm from the pile top to place anchor rods. The retaining plate is 1.66 m long, 1.5 cm thick, and 45 cm high. According to the experience, the dip angle of the bolt should be 15°-25° and should not be less than 10°. Accordingly, the dip angle of the bolt was set to 11°, 14°, and 18°. The anchorage cable No. 1, 2, and 3 with a diameter of 14 mm and a total length of 2.65 m, 2.12 m, and 1.68 m is connected to the antislide pile with an anchor cable angle of 11°, 14°, and 18°, respectively. One end of all bolts is connected to the bottom of the model box for anchorage, and the prestressing force applied on each bolt is 0.5 kN. The height, length, and width of the model box are 1.5 m, 3.5 m, and 1.66 m, respectively. The top view of the physical model is shown in Figure 1.

An acceleration sensor is arranged on the top of each pile to measure the acceleration and to convert the displacement of the pile top to electrical signals. Furthermore, strain gauges are arranged on four sides of the anchor cable 8 cm from the retaining plate to measure the applied axial force. Figures 2 and 3 show the assembly layout of acceleration sensors.

The studied seismic wave in this experiment is an El Centro wave as shown in Figure 4. Since the first seismic wave successfully records the whole process data, the El

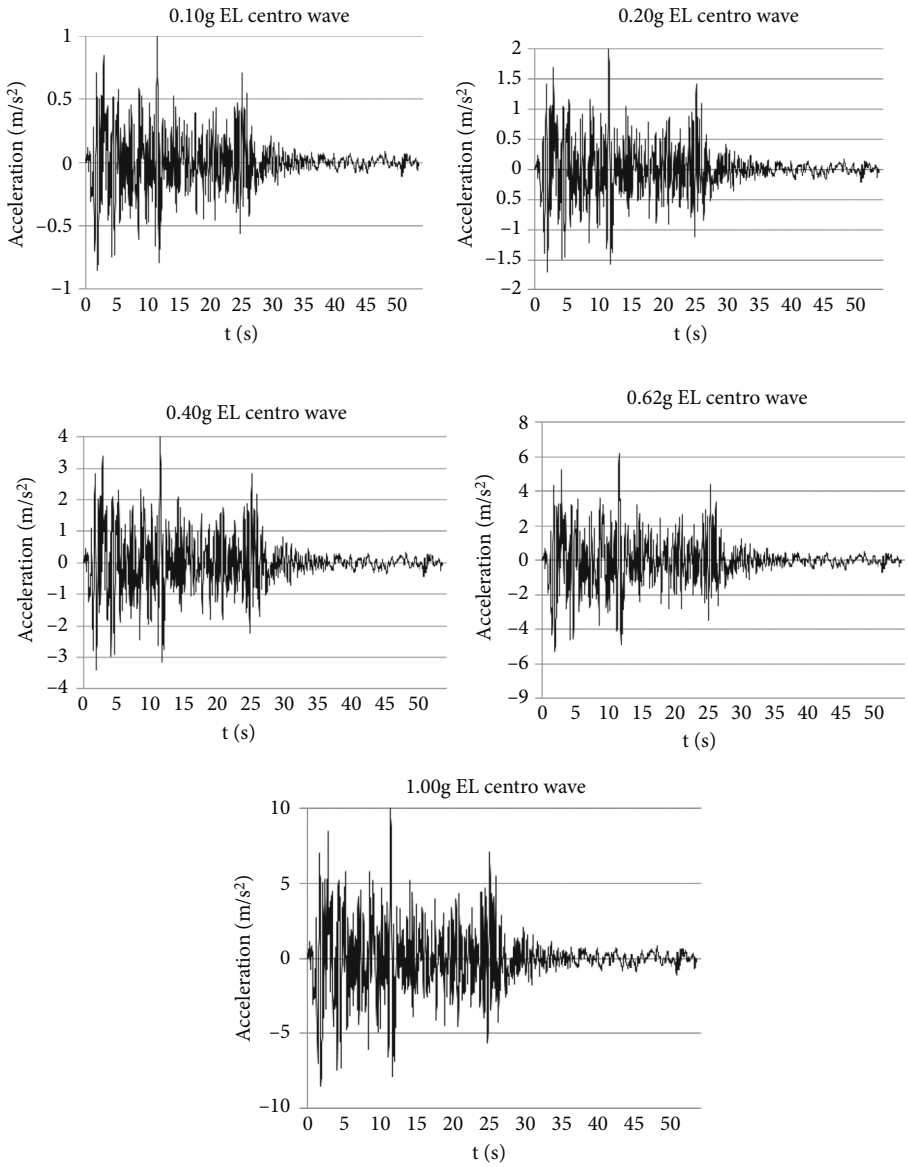


Figure 4: El Centro wave under five sets of conditions.

Centro wave is extensive and representative. In this regard, studies show that the horizontal component of the seismic wave is the fundamental force that causes the crack propagation, failure of the landslide, and its retaining structure. In the present study, five seismic conditions, including 7-degree medium earthquake, 8-degree medium earthquake, 8-degree large earthquake, 9-degree large earthquake, and over 9-degree earthquake, were designed. The control peak of the horizontal acceleration of these conditions is 0.10 g, 0.20 g, 0.40 g, 0.62 g, and 1.00 g, respectively. The data of slope acceleration, pile tip displacement, and anchor shaft force are collected in the test.

## 3. Analysis of the Test Results

*3.1. Seismic Displacement Response.* In the whole vibration process, the sensor monitoring data were analyzed mainly because the slope has been supported and no deformation failure occurred. Acceleration sensors A1, A2, and A3 were installed on the top of each antislide pile to measure the seismic acceleration response of the pile top under the action of the earthquake and obtain the time-history curves of pile top displacement under five working conditions. Figure 5 shows the displacement peaks of the pile top under pile-anchor system No. 1, 2, and 3. It is observed that as the earthquake power increases, the displacement of the pile top increases, and the response intensifies. Moreover, it is found that the displacement of the pile top increases rapidly before the acceleration of the seismic wave reaches 0.62 g, and then it increases slowly. The obtained results show that the aseismic effect of the anchor pile is remarkable.

Figure 6 shows the displacement of the pile top with different anchorage dip angles under the same seismic condition. It is observed that the displacement of the pile top

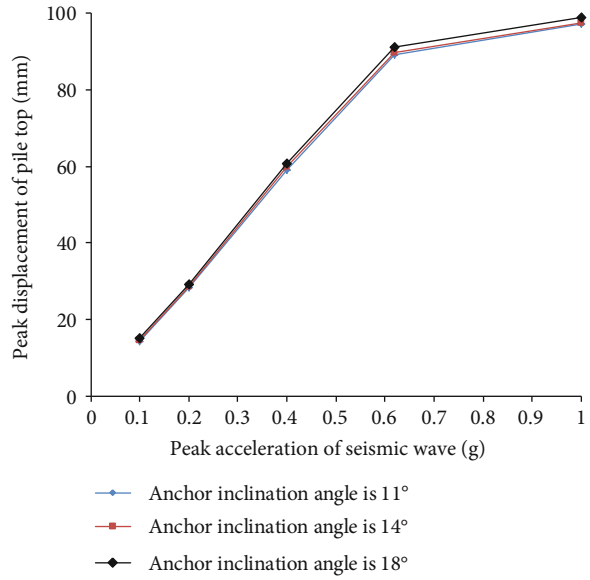


Figure 5: Peak displacement of the pile top under different working conditions.

with an 18° anchorage dip angle under the same seismic condition is larger than that of the pile top with a 14° anchorage dip angle. Meanwhile, the displacement of the pile top with a 14° anchorage inclination is always larger than that with an 11° anchorage inclination. It is concluded that as the anchorage angle increases, the corresponding displacement of the pile top increases too.

*3.2. Axial Force Response of the Anchor Rod.* The axial force peak values of three anchor cables with different inclination angles under different working conditions are presented in Figure 7.

Figure 7 shows that the axial force peak value of the anchor cable increases with the input seismic acceleration peak value, and the slope of the broken line of the axial force of each anchor cable becomes larger, indicating that the axial force grows faster and the response of the axial force intensifies.

The comparison of the axial force of the anchor cable under the same seismic condition with different inclination angles reveals that as the inclination angle increases, the corresponding axial force reduces continuously.

Table 2 shows the statistical tables of the peak values of the axial force and displacement of the anchor cable under the combined support of different pile-anchor systems. It is found that the axial force of the anchor cable is related to the displacement of the antislide pile under the pile-anchor combined support system. Figure 8 shows that under the same seismic conditions, the axial force of anchor rod No. 1 is greater than that of anchor rod No. 2 and 3, but the displacement of the pile top is just the opposite.

From the theoretical mechanics' viewpoint, the experimental results are in agreement with the theoretical ones. It is found that the angle between the pile and the anchor cable decreases with the increase of the inclination of the anchor cable and the decrease of the angle between the pile and the anchor cable. In this case, the seismic component of the anchor cable decreases, and the axial force of the anchor cable reduces, thereby weakening the pulling effect of the anchor cable and increasing the pile top displacement.

## 4. Validation of the Numerical Simulation

In this section, the flac3D software, which is a widely adopted software in geotechnical engineering, is applied to carry out numerical simulations. In this regard, three models are established, and each model has three antislide piles. The inclination angles of the three models are 11°, 14°, and 18°, respectively. In each model, the antislide pile in the middle position was selected for data analysis to avoid the influence of boundary conditions.

To increase the calculation accuracy and efficiency, the retaining plate, antislide pile, and anchor cable are treated as elastic materials. Table 3 shows the physical and mechanical parameters of model materials. Figure 9 shows that the established model is meshed using 5,634 elements and 9,789 nodes.

*4.1. Analysis of the Displacement Response of the Pile Top.* Three antislide piles are established in each model, and the time-history curve of the top displacement of middle antislide piles is selected for analysis. Figure 10 shows the distribution of the peak displacement of the pile top. It is observed that under the same seismic condition, the largest and smallest peak displacements of the pile top occur at an inclination angle of 18°and 11°, respectively. Furthermore, Figure 10 reveals that the peak displacement of the pile top increases with the increase of the anchor cable inclination. This is consistent with the obtained results from the shaking table test.

*4.2. Analysis of the Axial Force Response of the Anchor Cable.* Figure 11 shows the time-history curve of the axial force of the anchor cable at the same position at different anchor

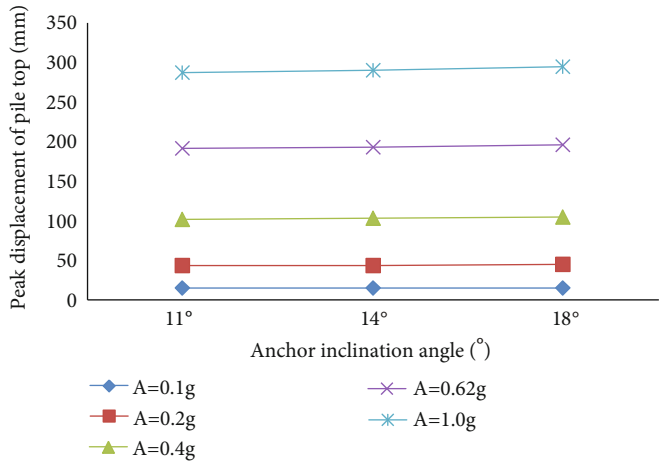


Figure 6: Distribution of the peak displacement of the pile top against the anchor inclination angle under the same working conditions.

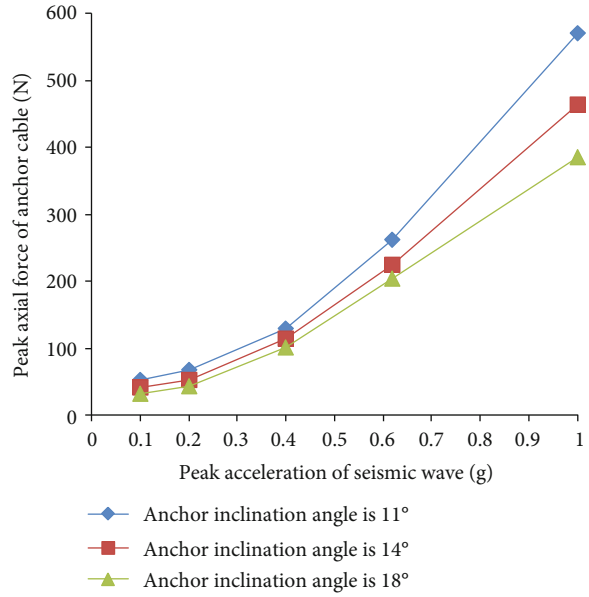


Figure 7: Peak axial force of the anchor cable under different working conditions.

Table 2: Axial force and peak displacement of anchor piles under different working conditions.

| Working conditions | Peak acceleration (g) | No. 1 | | No. 2 | | No. 3 | |
|---|---|---|---|---|---|---|---|
| | | Axial force (N) | Peak displacement (mm) | Axial force (N) | Peak displacement (mm) | Axial force (N) | Peak displacement (mm) |
| 1 | 0.1 | 51.73 | 14.42 | 40.33 | 14.61 | 31.41 | 15.03 |
| 2 | 0.2 | 67.43 | 28.45 | 53.27 | 28.69 | 42.18 | 29.22 |
| 3 | 0.4 | 129.01 | 59.09 | 114.23 | 59.79 | 100.99 | 60.78 |
| 4 | 0.62 | 261.41 | 89.16 | 224.15 | 89.75 | 204.75 | 91.29 |
| 5 | 1 | 571.15 | 97.09 | 464.01 | 97.38 | 384.88 | 98.99 |

inclination angles. It is observed that as the anchor inclination angle increases, the corresponding axial force decreases, which is in good agreement with the test results. It is also consistent with the theoretical deduction that the higher the inclination of the anchor cable, the lower the intersection angle between the pile and the anchor cable, the smaller the seismic component of the anchor cable, the lower the axial force of the anchor cable, and the weaker the anchor cable.

*4.3. Response Analysis of Dynamic Earth Pressure behind the Pile.* In this section, the dynamic earth pressure along the $x$-axis behind the anchored pile is monitored. During the

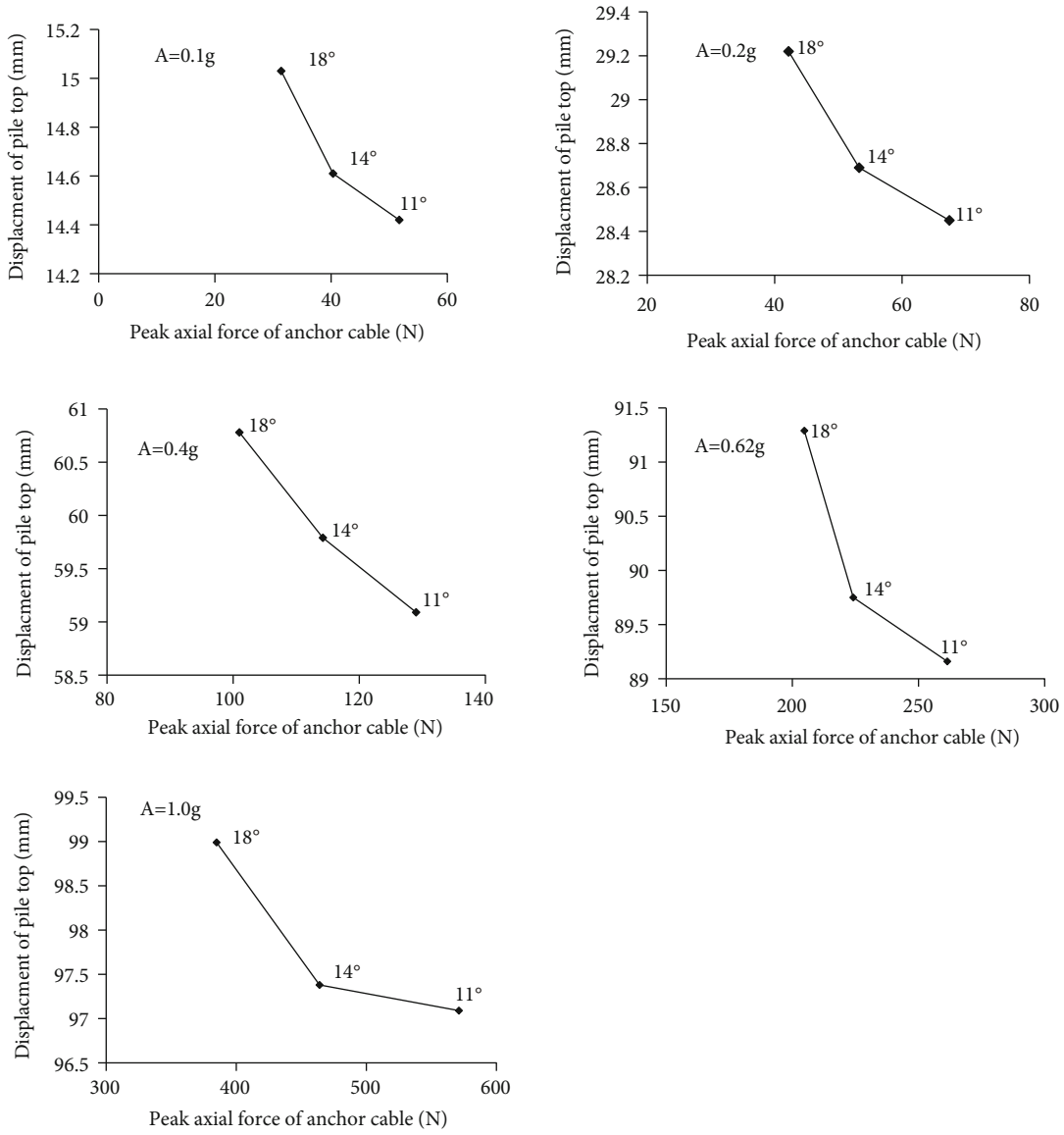


Figure 8: Distribution of axial force of the anchor cable against the pile top displacement.

Table 3: Physical and mechanical parameters of model materials.

| Material | $r$ kN/m$^3$ | $Es$ MPa | $\mu$ | Notes |
|---|---|---|---|---|
| Retaining plate | 22 | 1.2*E*3 | 0.35 | |
| Antislide pile | 23 | 3.0*E*3 | 0.30 | Elastic material |
| Anchor rod | 78 | 2.0*E*4 | 0.20 | |

analysis, the earth pressure increased in the process of earthquake action, without considering the earth pressure under static action. Therefore, monitoring points are set after the initial balance to monitor the variations of the earth pressure behind the antislide piles when applying seismic waves. In this simulation, a total of 9 monitoring points are set up, and 3 points are set after each pile. Figure 12 shows that the monitoring points are set at 20 cm intervals above the sliding surface.

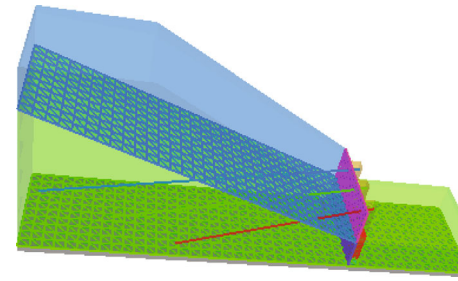

Figure 9: Three-dimensional model of the anchor pile.

In this analysis, 0.35 g El Centro waves are considered as the input seismic waves. Figures 13–15 show the time-history curves of the dynamic earth pressure behind the piles detected at W1, W2, and W3 of antislide piles No. 1, 2, and 3, respectively.

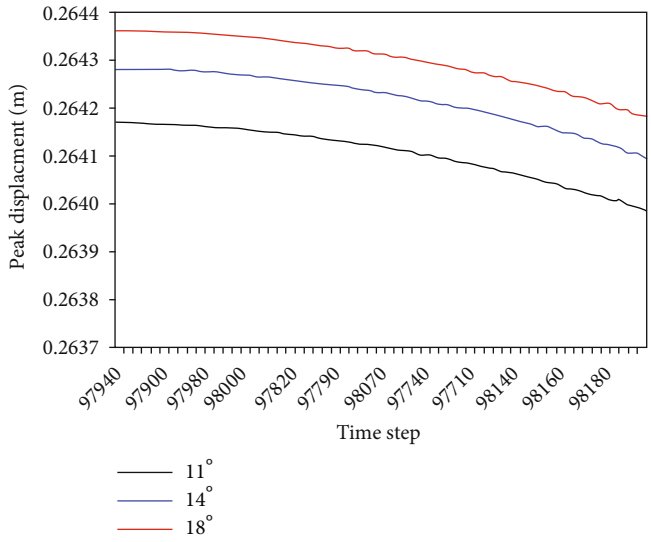


Figure 10: Distribution of the maximum displacement peak against the calculation time step.

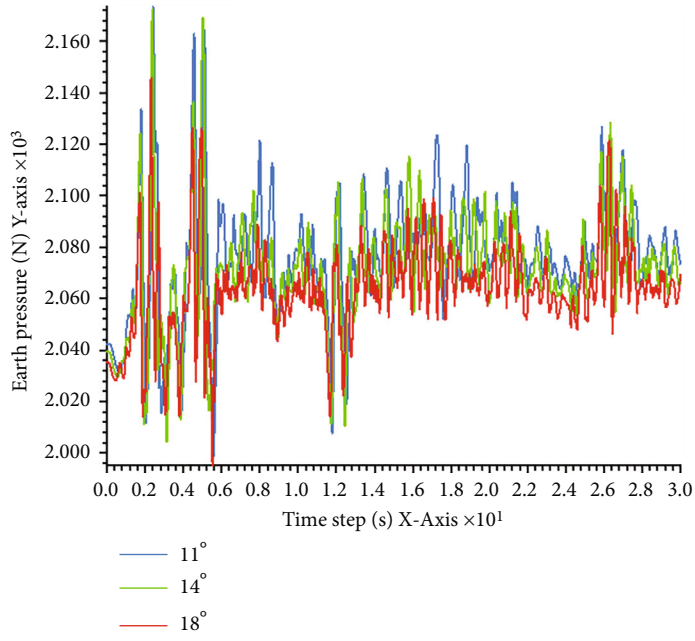


Figure 11: Distribution of the anchor cable axial force under different anchor angles.

The comparison of time-history curves of the dynamic earth pressure at different heights after three antislide piles indicates that the properties of the dynamic earth pressure behind piles change from the sliding surface to the top of the pile. More specifically, the dynamic earth pressure near the sliding surface (W1) is active, while the dynamic earth pressure near the pile top (W2, W3) is passive. This is because W1 is located near the sliding surface, so it is subjected to a large thrust of the sliding body of the pile, while W2 and W3 are subjected to the reverse pressure on the soil because of the anchor pulling action. Meanwhile, W3 is near the pile top, where the largest anchor pulling action and the biggest passive earth pressure occur.

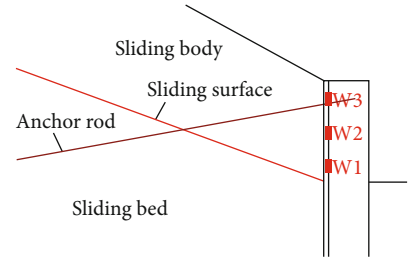


Figure 12: The monitoring points of dynamic earth pressure at postpile.

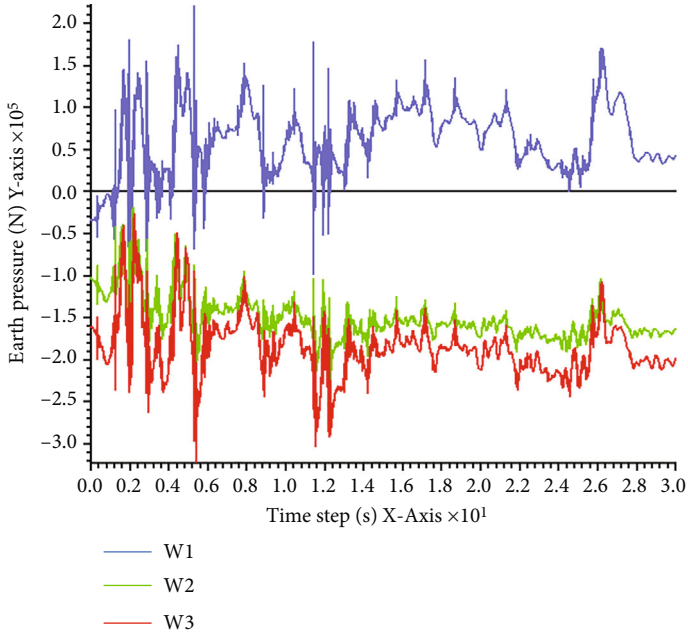


Figure 13: The time-course curve of the earth pressure behind the antislide pile No. 1.

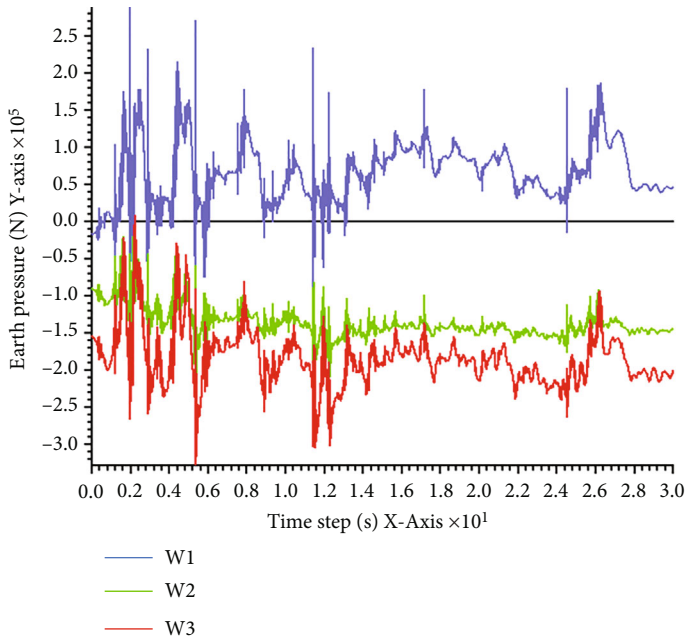


Figure 14: The time-course curve of the earth pressure behind the antislide pile at No. 2.

The distributions of the earth pressure behind the pile at the same location with different anchorage angles are shown in Figures 16–18. It is observed that variations of different anchor inclination angles at the same position are basically the same. It is found that as the anchorage angle increases, the active earth pressure increases, and the passive earth pressure decreases near the pile top. This is because as the inclined angle of the anchor cable increases, the intersection angle of the pile and the anchor cable decreases, the seismic component of the anchor cable reduces, the effect of the anchor cable weakens, and the passive earth pressure of the pile on the soil reduces. The obtained results verify the relationship between the displacement of the pile top and the anchorage dip angle.

## 5. Conclusion

In the present study, a large-scale model test platform was used to investigate the seismic response characteristics of anchor piles with different slope angles of anchor cables. Based on the obtained results, the main achievements can be summarized as follows:

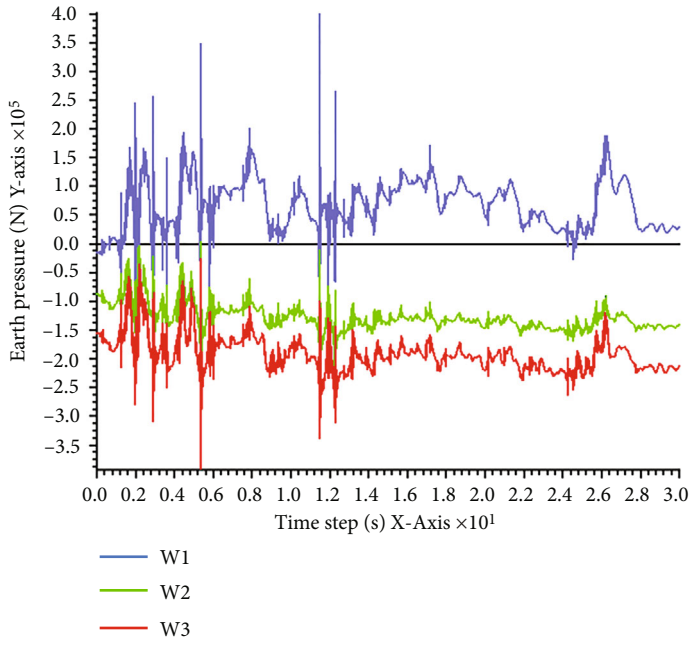


Figure 15: The time-course curve of the earth pressure behind the antislide pile No. 3.

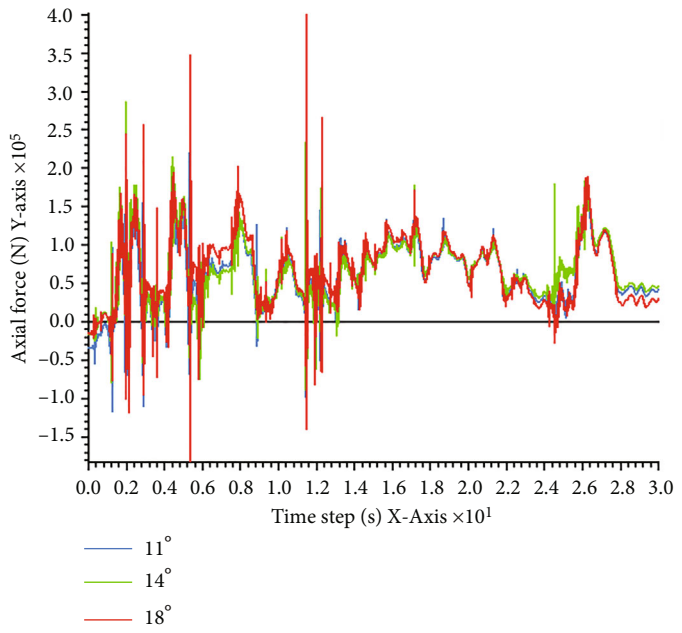


Figure 16: Distribution of dynamic earth pressure at W1 under different anchor angles.

(1) The inclined angle of the anchor cable has a great influence on the seismic response of the pile-anchor system. As the inclined angle of the anchor cable increases, the axial force of the seismic response decreases while the displacement of the pile top increases. Moreover, as the inclination of the anchor cable increases, the intersection angle of the pile and the anchor cable decreases, the seismic component of the anchor cable decreases, the axial force of the anchor cable decreases, the effect of the anchor cable on the piles weakens, and the pile top displacement increases

(2) With the increase of the earthquake power, the peak displacement of the pile top and the axial force of the anchor cable increase, and the seismic response

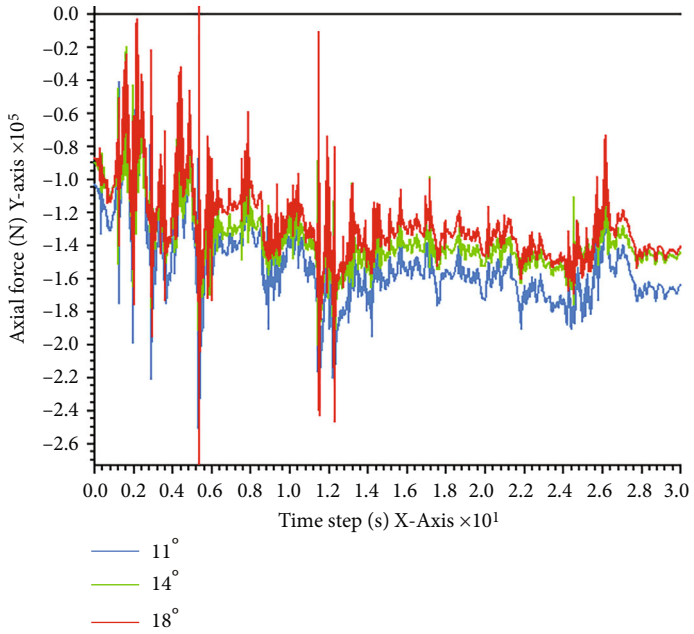


Figure 17: Distribution of dynamic earth pressure at W2 under different anchor angles.

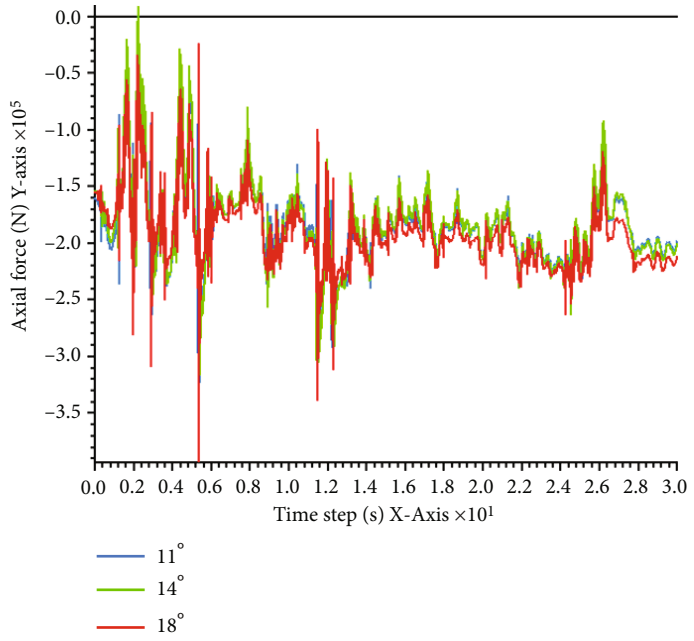


Figure 18: Distribution of dynamic earth pressure at W3 under different anchor angles.

intensifies. Accordingly, when the acceleration of the seismic wave is less than 0.62 g, the pile top displacement increases rapidly. However, when the earthquake power exceeds 0.62 g, the displacement increases slowly

(3) The performed numerical simulation shows that the dynamic earth pressure of anchor piles is active near the sliding surface and increases with the increase of the anchor dip angle. Moreover, it is passive at the pile top and decreases with the increase of the anchor dip angle. This is because with the increase of the inclined angle of the anchor cable, the intersection angle of the pile and the anchor cable decreases, the seismic component of the anchor cable reduces, the effect of the anchor cable weakens, and the passive earth pressure of the pile to the soil reduces. Accordingly, the correlation between the pile top displacement and the angle of the anchor cable is verified

## Data Availability

The data used to support the findings of this study are included within the article.

## Conflicts of Interest

The authors declare that they have no conflicts of interest.

## Authors' Contributions

A.Fayou and Xue-gang Dai contributed equally to this work.

## Acknowledgments

The authors acknowledge the National Natural Science Foundation of China (Grant: 41562016), the General Project of Yunnan Applied Basic Research Plan (Grant: 2017FB070), and the Key Research and Development Program of Yunnan Province in 2022 (the technology and application of integrated risk assessment for major earthquake disasters and their disaster chains in Yunnan).

## References

[1] B. M. Das and V. K. Puri, "Holding capacity of inclined square plate anchors in clay," *Soils and Foundations*, vol. 29, no. 3, pp. 138–144, 1989.

[2] P. K. Basudhar and D. N. Singh, "A generalized procedure for predicting optimal lower bound break-out factors of strip anchors," *Geotechnique*, vol. 44, no. 2, pp. 307–318, 1994.

[3] D. K. Keefer, "Statistical analysis of an earthquake-induced landslide distribution – the 1989 Loma Prieta, California event," *Engineering Geology*, vol. 58, no. 3-4, pp. 231–249, 2000.

[4] G. A. O. Da-shui and Z. E. N. G. Yong, "Monitoring analysis of pre-stress state of anchor cable of high slope in the TGP permanent ship locks," *Chinese Journal of Rock Mechanicsand Engineering*, vol. 20, no. 5, pp. 653–656, 2001.

[5] L. I. Ning, Z. Peng, and Y. Chong, "Research on stability of left abutment slope of Jinping hydro-power station and reinforcement measurements of pre-stressed anchorage cable," *Chinese Journal of Rock Mechanics and Engineering*, vol. 26, no. 1, pp. 36–42, 2007.

[6] P. Bhattacharya, "Pullout capacity of shallow inclined anchor in anisotropic and nonhomogeneous undrained clay," *Geomechanics & Engineering*, vol. 13, no. 5, pp. 825–844, 2017.

[7] P. Bhattacharya and S. Sahoo, "Uplift capacity of horizontal anchor plate embedded near to the cohesionless slope by limit analysis," *Geomechanics & engineering*, vol. 13, no. 4, pp. 701–714, 2017.

[8] D. P. Zhou, J. J. Zhang, and Y. Tang, "Seismic damage analysis of road slopes in Wenchuan earthquake," *Chinese Journal of Rock Mechanics and Engineering*, vol. 29, no. 3, pp. 565–576, 2010.

[9] Z. H. E. N. G. Tong, L. I. U. Hongshuai, Y. U. A. N. Xiaoming, and Q. I. Wenhao, "Experimental study on seismic response of anti-slide piles with anchor cables by centrifugal shaking table," *Chinese Journal of Rock Mechanics and Engineering*, vol. 35, no. 11, pp. 2276–2286, 2016.

[10] A. J. Valsangkar, J. L. Dawe, and K. A. Mita, "Shake hake table studies of seismic response of single partially supported piles," in *6TH Canadian Conf on Earthquake Engineering*, Toronto, Canada, June 1991.

[11] N. Makris and D. Badoni, "Nonlinear seismic response of single piles," in *7th International Conference on Soil Dynamics and Earthquake Engineering (SDEE 95)*, Crete, Greece, May 1995.

[12] H. Yi, H. Hemanta, Y. Noriyuki, H. Zheng, and L. Yang, "Three-dimensional limit analysis of seismic displacement of slope reinforced with piles," *Soil Dynamics & Earthquake Engineering*, vol. 77, pp. 446–452, 2015.

[13] E. Sáez, G. S. Pardo, and C. Ledezma, "Seismic response of a pile-supported excavation on Santiago gravel," *Soil Dynamics and Earthquake Engineering*, vol. 76, pp. 2–12, 2015.

[14] Q. Honglue, L. Ying, H. Luo Hao, and H.,. H. Qindi, "Seismic response characteristics of stabilizing pile based on elastic-plastic analysis," *Shock & Vibration*, vol. 2018, pp. 1–15, 2018.

[15] L. Nan, Y. Me, Y. Liqun, W. Banqiao, L. Jun, and L. Xueling, "Seismic response of micropiles-reinforced landslide based on shaking table test," *Geomatics, Natural Hazards and Risk*, vol. 10, no. 1, pp. 2030–2050, 2019.

[16] C. Zhang, G. Jiang, L. Su, W. L. Da Lei, and Z. Wang, "Large-scale shaking table model test on seismic performance of bridge-pile-foundation slope with anti-sliding piles: a case study," *Bulletin of Engineering Geology & the Environment*, vol. 79, no. 3, pp. 1429–1447, 2020.

[17] S. Hua-you and Z. Ji-chun, "Analysis of blastingvibration effect on pre-stressed cable of high slope in Zipingpu project," *Chinese Journal of Rock Mechanics and Engineering*, vol. 22, no. 11, pp. 1916–1918, 2003.

[18] S. H. Yang, B. Liang, J. C. Gu, J. Shen, and A. M. Chen, "Research on characteristics of prestress change of anchorage cable in anti-expulsion model test of anchored cavern," *Chinese Journal of Rock Mechanics and Engineering*, vol. 25, no. S2, pp. 3749–3756, 2006.

[19] H. L. Ye, Y. R. Zheng, A. H. Li, and X. Du, "Shaking table test studies of pre-stressed anchor cable of slope under earthquake," *Chinese Journal of Rock Mechanics and Engineering*, vol. 31, no. S1, pp. 2847–2854, 2012.

[20] J. Xu, Y. Zheng, and F. Wu, "Research on interaction between the embedded anti-slide piles and the frame beam with pre-stressed anchors," in *2014 Geo Shanghai International Congress: Advances in Soil Dynamics and Foundation Engineering*, Shanghai, China, May 2014.

[21] H. Qu, J. J. Zhang, and F. Wang, "Seismic response of pre-stressed anchor sheet pile wall from shaking table tests," *Chinese Journal of Geotechnical Engineering*, vol. 35, no. 2, pp. 313–320, 2013.

[22] W. Zhou, L. I. Hai-bo, and Y. Liu, "Pseudo-dynamic analysis of anchored characteristics of layered rock slopes subjected to seismic loads," *Chinese Journal of Rock Mechanics and Engineering*, vol. 35, no. S2, pp. 3570–3576, 2016.

[23] Y. Min-jia, X. Yuan-you, and L. Ting-ting, "Limit analysis of bedding rock slopes reinforced by prestressed anchor cables under seismic loads," *Rock and Soil Mechanics*, vol. 39, no. 7, pp. 2091–2698, 2018.

[24] X. Fu, J. Zhang, W. Liao, L. Cao, and G. Fan, "Shaking table test on seismic response of slopes reinforced by pile-cable retaining structure," *Yanshilixue Yu Gongcheng Xuebao/Chinese Journal*

*of Rock Mechanics and Engineering*, vol. 36, no. 4, pp. 831–842, 2017.

[25] C. Fumao, T. Huiming, C. Jia, and J. Zhibin, "Influences of earthquake characteristics on seismic performance of anchored sheet pile quay with barrette piles," in *15th International Coastal Symposium (ICS)*, Busan, South Korea, May 2018.

[26] L. Yu-liang, C. Xue-ming, and Y. Guo-lin, "Seismic response of a sheet-pile wall with anchoring frame beam by numerical simulation and shaking table test," *Soil Dynamics and Earthquake Engineering*, vol. 115, pp. 352–364, 2018.

[27] Y. Huang, X. Xi, and L. Junji, "Centrifuge modeling of seismic response and failure mode of a slope reinforced by a pile-anchor structure," *Soil Dynamics & Earthquake Engineering*, vol. 131, article 106037, 2020.

[28] L. Xianqi and G. Xiurun, *Theory and Application of Model Test and Landslide*, China Waterpower Press, Beijing, China, 2008.